第 29 卷第 7 期 无 机 化 学 学 报 Vol.29 No.7
2013 年 7 月 CHINESE JOURNAL OF INORGANIC CHEMISTRY 1490-1496

基于面式–三(2-(4-三氟甲基苯基)吡啶)合铱配合物为发光中心的高效绿光有机电致发光器件

滕明瑜 王铖铖 荆一铭 郑佑轩* 林 晨*
(南京大学化学化工学院,配位化学国家重点实验室,南京微结构国家实验室(筹),南京 210093)

摘要: 用经典的方法合成了面式–三(2-(4-三氟甲基苯基)吡啶)合铱配合物(*fac*-Ir(tfmppy)$_3$),并得到了其晶体结构。在 CH_2Cl_2 溶液中 Ir(tfmppy)$_3$ 的发射光谱显示出了峰值位于 525 nm 的 $\pi\rightarrow\pi^*$ 跃迁吸收以及金属到配体电荷转移(MLCT)吸收,色坐标(CIE)为(0.31,0.62),量子效率计算为 4.59%(以 Ru(bpy)$_3$]Cl$_2$ 为参照)。以 Ir(tfmppy)$_3$ 为发光中心,制备并研究了有机电致发光器件:ITO/TAPC (60 nm)/Ir(tfmppy)$_3$ (*x*%):mCP (30 nm)/TPBi (60 nm)/LiF (1 nm)/Al (100 nm)。4%掺杂浓度的器件在 4 197 cd·m^{-2} 的亮度下显示的最大电流效率为 33.95 cd·A^{-1},在 12.7 V 时的最大亮度为 43 612 cd·m^{-2},色坐标(CIE)为(0.31,0.61)。利用瞬态电致发光法(transient electroluminescence (TEL))、在 1 300 (V·cm^{-1})$^{1/2}$ 的电场强度下 Ir(tfmppy)$_3$ 配合物的电子迁移率测定为 4.24×10^{-6} cm^2·(V·s)$^{-1}$。非常接近于常用的电子传输材料八羟基喹啉铝(Alq$_3$)的电子迁移率。

关键词: 铱配合物; 4-三氟甲基苯联吡啶; 电致磷光; 有机电致发光; 电子迁移率
中图分类号: O641.825 **文献标识码**: A **文章编号**: 1001-4861(2013)07-1490-07
DOI:10.3969/j.issn.1001-4861.2013.00.236

Efficient Green Organic Light-Emitting Diodes with *fac*-Tris(2-(4-trifluoromethylphenyl)pyridine)iridium Complex as Emitter

TENG Ming-Yu WANG Cheng-Cheng JING Yi-Ming ZHENG You-Xuan* LIN Chen*
(*State Key Laboratory of Coordination Chemistry, Nanjing National Laboratory of Microstructures, School of Chemistry and Chemical Engineering, Nanjing University, Nanjing* 210093, *China*)

Abstract: *fac*-Tris(2-(4-trifluoromethylphenyl)pyridine)iridium (Ir(tfmppy)$_3$) was prepared by conventional method and its crystal structure was determined. Excitation at either $\pi\rightarrow\pi^*$ or MLCT absorption band of Ir (tfmppy)$_3$ in CH_2Cl_2 solution leads to the same MLCT emission maxima at 525 nm with Commission Internationale de L′Eclairage (CIE) coordinates of (0.31, 0.62) and the emission quantum yield is 4.59% in CH_2Cl_2 (by reference to an aerated aqueous solution of [Ru (bpy)$_3$]Cl$_2$ as the standard solution). Organic light-emitting diodes (OLEDs) based on the green electrophosphorescent complex in ITO/TAPC (1,1-bis [4-[*N*,*N*-di(p-tolyl)amino]phenyl]cyclohexane, 60 nm)/Ir(tfmppy)$_3$ (*x*%):mCP (1,3-bis (carbazol-9-yl)benzene, 30 nm)/TPBi (2,2′,2″-(1,3,5-benzinetriyl)-tris(1-phenyl-1-*H*-benzimidazole, 60 nm)/LiF (1 nm)/Al (100 nm) were investigated. The device with 4% dopant concentration shows a maximum current efficiency of 33.95 cd·A^{-1} at 4 197 cd·m^{-2}, a maximum brightness of 43 612 cd·m^{-2} at 12.7 V, and CIE coordinates of (0.31, 0.61). The device with 6% dopant concentration exhibits a maximum power efficiency of 27.29 cd·A^{-1} at 1 981 cd·m^{-2}, a maximum brightness of 33 071 cd·m^{-2} at 9.6 V. The electron mobility of Ir(tfmppy)$_3$ is 4.24×10^{-6} cm^2·(V·s)$^{-1}$ under electric field of 1 300 (V·cm^{-1})$^{1/2}$ via transient electroluminescence (TEL) method, which is close to that of Alq$_3$ (tri(8-hydroxyquinoline)aluminum) emitter. CCDC: 887658.

Key words: iridium complex; 2-(4-trifluoromethylphenyl)pyridine; electrophosphorescence; organic light-emitting diodes; electron mobility

收稿日期:2012-12-24。收修改稿日期:2013-04-01。
国家自然科学基金(No.20971067)和江苏省自然科学基金(No.BK2011551)资助项目。
*通讯联系人。E-mail:yxzheng@nju.edu.cn,linchen@nju.edu.cn

0 Introduction

In the last decades, high efficient electrophosphorescence from iridium(Ⅲ)-based complexes, such as $Ir(piq)_3$ (piq=1-phenylisoquinolato)[1-2], $Ir(ppy)_3$ (ppy=2-phenylpyridine)[3], FIrpic (iridium(Ⅲ) bis[(4,6-difluorophenyl)-pyridinato-*N*,C_2] picolinate)[4-5], and so on[6-13], foreshadowed a breakthrough in organic light-emitting diodes (OLEDs). Cyclometalated Ir(Ⅲ) complexes show brilliant luminescence due to their strong triplet emission with high phosphorescent efficiencies caused by strong spin-orbit coupling[14-15].

fac-$Ir(ppy)_3$ has been reported as highly efficient phosphorescent OLEDs material due to its short triplet lifetime and reasonable photoluminescent performance[16-20]. *fac*-$Ir(tfmppy)_3$ (tfmppy =2-(4-trifluoromethylphenyl)pyridine) with a strong electron-withdrawing group-CF_3 attached to the ppy ligand exhibits efficient photoluminescence (PL). In 1990, Watts et al[21] first reported the synthesis and PL properties of $Ir(tfmppy)_3$ complex. In 2011, Michael et al[22] reported the synthesis and PL of a series of Ir/Eu dyads, and one complex containing tfmppy ligand. Yu et al[23] reported two charge-neutral amidinate and tfmppy ligand containing iridium complexes capable of efficient photocatalytic water reduction. Our group [24-25] reported the electroluminescence (EL) prop-erties of iridium complexes with 2-(4-trifluoromethyl-phenyl) pyridine as main ligands with good performa-nces. For example, the device using $Ir(tfmppy)_2tpip$ (tpip= tetraphenylimidodiphosphinate) as the emitter has a maximum luminance of 64 351 $cd\cdot m^{-2}$ at 11.8 V with a maximum current efficiency (η_c) of 67.95 $cd\cdot A^{-1}$ and a maximum power efficiency (η_p) of 69.90 $lm\cdot W^{-1}$, respectively[24].

But till now, to the best of our knowledge, there still has been no report on the electroluminescence (EL) performance of this complex. In this work, we construct some devices employing fac-$Ir(tfmppy)_3$ as green electrophosphorescent emitter. The CF_3 group is considered to have several advantages in improving the device performance[12,26-27]: (i) lower vibrational frequency of C-F bond can reduce the rate of radiationless deactivation; (ii) the bulky CF_3 substituents can affect the molecular packing and the steric protection around the metal can suppress the self-quenching behavior; (iii) fluorination can enhance the electron mobility and result in better balance of charge injection and transfer. Tfmppy used as ligand may shorten the lifetime of excitation and affect the emission wavelength, then further improve the OLEDs performances.

1 Experimental

1.1 Materials and characterization

The other organic materials used in this study were obtained commercially and used as received. The absorption spectrum and PL/EL spectra were measured with a Shimadzu 3600 and Hitachi F-4600, respectively. The voltage-luminance (*V-L*) characteristics and current efficiency (η_c) versus *J* curves of the devices were measured by a computer controlled KEITHLEY 2400 source meter with a calibrated silicon diode in air. The η_c is the way to represent the ratio of the luminance to the current density flowing into the device and is expressed as $cd\cdot A^{-1}$. The power efficiency (η_p) is the ratio of the optical flux to the electrical input and is expressed as $lm\cdot W^{-1}$. On the basis of the uncorrected PL and EL spectra, the Commission Internationale de l′clairage (CIE) coordinates were calculated using a test program of the spectra scan PR650 spectrophotometer.

1.2 Synthesis of fac-$Ir(tfmppy)_3$

fac-$Ir(tfmppy)_3$ was prepared in 2-ethoxyethanol using $[(tfmppy)_2Ir(\mu\text{-}Cl)]_2$, potassium carbonate and tfmppy as starting materials (Scheme 1) according to the published literatures[2,15].

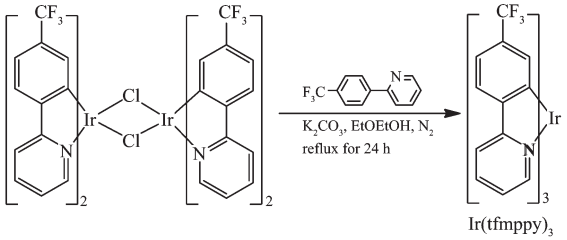

Scheme 1　Synthetic route of the complex $Ir(tfmppy)_3$

1.2.1 Synthesis of 2-(4-(trifluoromethyl)phenyl) pyridine (tfmppy)

A 250 mL three-necked round-bottomed flask was charged with 2-(4-trifluoromethyl)-phenylboronic acid (8.55 g, 45.0 mmol), MeOH (40 mL), and an aqueous solution of Na_2CO_3 (2 mol·L^{-1}, 60 mL) under a N_2 atmosphere. The mixture was refluxed and stirred vigorously. After 5 min 2-bromopyridine (3.76 mL, 40.0 mmol), $Pd(PPh_3)_4$ (0.519 g, 0.45 mmol) and MeOH (60 mL) were added. After the reaction was complete (controlled by TLC), the reaction mixture was cooled and the solvents were removed in vacuum to give the crude product. The crude product was purified by column chromatography (neutral alumina; petroleum ether:EtOAc=4:1, *V*/*V*) to give yellow color liquid (7.6 g, 33.6 mmol) in 84% yield. ^{1}H NMR (500 MHz, $CDCl_3$, ppm) δ=8.73 (d, *J*=4.7 Hz, 1H), 8.31 (d, *J*=8.1 Hz, 2H), 8.07 (d, *J*=8.0 Hz, 1H), 7.94 (td, *J*=7.8, 1.8 Hz, 1H), 7.84 (d, *J*=8.3 Hz, 2H), 7.44 (ddd, *J*=7.4, 4.8, 0.8 Hz, 1H). MALDI-TOF: Calcd. [M$^+$] 223.19; Found [M$^+$] 223.41.

1.2.2 Synthesis of $[(tfmppy)_2Ir(\mu\text{-}Cl)]_2$

$IrCl_3·3H_2O$ (0.53 g, 1.5 mmol) and tfmppy (0.76 g, 3.4 mmol) were refluxed in 10 mL $EtOCH_2CH_2OH$/H_2O (3:1, *V*/*V*) at 140 ℃ for 20 h. After cooling down, yellow precipitate was filtered and washed with petroleum ether. The washed product was dried under vacuum with a 84% yield (0.84 g, 0.50 mmol). MALDI-TOF: Calcd. [M$^+$] 1 344.08; Found [M$^+$] 1 344.54.

1.2.3 Synthesis of $Ir(tfmppy)_3$

$[(tfmppy)_2Ir(\mu\text{-}Cl)]_2$ (0.672 g, 0.50 mmol) and 2.5 equivalent tfmppy (0.34 g, 1.25 mmol) were dissolved in 10 mL of $EtOCH_2CH_2OH$. After degassing, the reaction solution was maintained at 140 ℃ for 12 hr under nitrogen. The crude compound was filtered after the solution cooling to room temperature and dried under vacuum. Further purification was taken by gradient sublimation with a yield of 0.18 g (0.21 mmol, 21%), m.p. > 250 ℃. ^{1}H NMR (500 MHz, DMSO-d_6) δ=8.40 (d, *J*=8.0 Hz, 1H), 8.30 (t, *J*=8.5 Hz, 2H), 8.12 (dd, *J*=17.0, 8.5 Hz, 2H), 8.04 (d, *J*=8.0 Hz, 1H), 7.97~7.88 (m, 3H), 7.85 (t, *J*=7.5 Hz, 1H), 7.79 (d, *J*=5.0 Hz, 1H), 7.68 (d, *J*=5.5 Hz, 1H), 7.32 (t, *J*=6.0 Hz, 1H), 7.26 (t, *J*=8.5 Hz, 2H), 7.22~7.17 (m, 3H), 6.87 (s, 1H), 6.63 (s, 1H), 6.49 (s, 1H). ^{13}C NMR (125 MHz, DMSO-d_6) δ=175.5, 173.7, 168.2, 166.0, 165.6, 158.1, 152.7, 150.0, 149.3, 148.6, 147.1, 138.9, 138.3, 136.9, 132.3, 130.0~129.1 (m), 127.6, 126.2 (d), 125.8 (d), 125.3, 125.2, 125.1, 125.0, 124.6, 124.0 (d), 123.7, 121.6, 121.3, 119.0, 118.7, 116.6. MALDI-TOF, *m*/*z*: [M] Calcd. for $C_{36}H_{21}IrF_9N_3$, 858.77; Found, 859.24 [M], 634.92 [M-224].

1.3 Fabrication of OLEDs

With the aim of evaluating the EL performance, $Ir(tfmppy)_3$ was used as the guest material in devices of ITO/TAPC (1,1-bis[4-[*N*,*N*-di(p-tolyl)amino]phenyl] cyclohexane, 60 nm)/$Ir(tfmppy)_3$ (*x*%):mCP (1,3-bis (carbazol-9-yl)benzene, 30 nm)/TPBi (2,2′,2″-(1,3,5-benzinetriyl)-tris(1-phenyl-1-H-benzimidazole, 60 nm)/LiF (1 nm)/Al (100 nm). TAPC film was designed as a hole transport layer (HTL), $Ir(tfmppy)_3$ doped mCP was applied as an emissive layer (EML), and a thin TPBi layer was deposited as the electron transport layer (ETL) and hole block layer (HBL). Indium-tin oxide (ITO) coated glass with a sheet resistance of 25 Ω/sq was used as the anode substrate. Substrates were cleaned by ultrasonic baths in organic solvents and de-ionized water followed by ozone treatment for 20 min and then oxygen plasma for 10 min at pressure of 10 to 20 Pa to enhance the surface work function of ITO anode (from 4.7 to 5.1 eV)[28]. All the organic layers were deposited at a rate of 0.1 nm·s^{-1} under high vacuum (less than 2×10^{-4} Pa). LiF and Al were deposited in another vacuum chamber (less than 3×10^{-4} Pa) with rates of 0.02 and 1 nms^{-1}, respectively. The evaporation rate of individual material and the thicknesses of layers were monitored in vacuum with quartz crystal monitors. A shadow mask was used to define the cathode and to make 0.1 cm^2 devices on each substrate.

2 Results and discussion

2.1 Crystallography of fac-$Ir(tfmppy)_3$

The crystal structure of $Ir(tfmppy)_3$ and the crystal data are shown in Fig.1. The iridium center is octahedrally coordinated by three bidentate C^N ligands. The average bond length of Ir-C and Ir-N is 0.202 3(13) and 0.209 0(12) nm, respectively. The

average angle of C-Ir-N is 77.6 (4)°. All other bond lengths and angles are within the normal values for cyclometalated ppy to Ir(Ⅲ) center. The X-ray data show that the dihedral angle [C(25)-C(30)-C(32)-C(36)] between phenyl ring and pyridinyl ring is −179.954 (132)°, which indicates those two rings are almost coplanar.

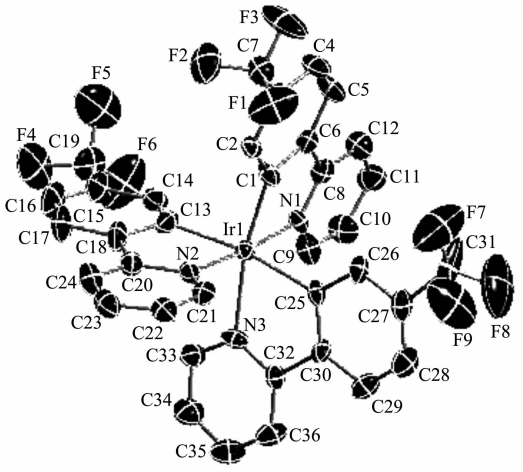

Fig.1　Oak Ridge Thermal Ellipsoidal plot (ORTEP) diagram of Ir(tfmppy)$_3$, Thermal ellipsoids are drawn at a 30% probability level, All hydrogen atoms are omitted for clarity

Crystal data: $C_{36}H_{21}IrF_9N_3$, M_w=858.78, monoclinic, space group $P2_1/c$, a=1.200 36(15) nm, b=3.491 2(4) nm, c=1.761 65(17) nm, $\alpha=\gamma=90°$, β=120.098(6), V=6.387 1 (12) nm^3, Z=8, D_c=1.786 g·cm^{-3}, μ (Mo $K\alpha$) (mm^{-1}): 4.265, F(000)=3 327, GOF=0.877, R_1=0.067 0, wR_2=0.153 3. Selected bond lengths (nm): C(1)-Ir(1): 0.200 3(10), N(1)-Ir(1): 0.206 7(8), C(13)-Ir(1): 0.208 8(11), N(2)-Ir(1): 0.203 6(9), N(3)-Ir(1): 0.217 7(8), C(25)-Ir(1): 0.207 5(11). Selected angles (°): C(1)-Ir(1)-N(1): 81.0(4), C(1)-Ir(1)-N(2): 95.7(4), C(25)-Ir(1)-N(3): 77.5(4), C(13)-Ir(1)-N(2): 80.2(4), C(13)-Ir(1)-N(3):94.0 (4), C(1)-Ir(1)-C(25): 91.9(5).

CCDC: 887658.

2.2　UV-Vis spectra and photoluminescence property

The UV-Vis absorption, emission spectra of Ir(tfmppy)$_3$ in CH_2Cl_2 solution and solid state at room temperature are displayed in Fig.2. Ir(tfmppy)$_3$ exhibits intense UV absorption bands due to the spin-allowed ligand centered (ancillary ligand) transitions at higher energies before 380 nm, while an admixture of metal-to-ligand charge transfer states (MLCT) appears at lower energies after 400 nm with lower extinction coefficients.

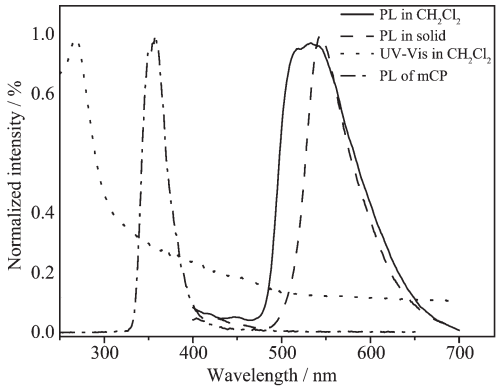

Fig.2　Absorption and emission spectra of Ir(tfmppy)$_3$ recorded in CH_2Cl_2 solution or in solid state, and emission spectrum of mCP in CH_2Cl_2 solution at 298 K

Excitation at either $\pi\rightarrow\pi^*$ absorption band or MLCT absorption band of Ir(tfmppy)$_3$ in CH_2Cl_2 solution leads to the same MLCT emission maxima at 525 nm (green color, x=0.31, y=0.62 of CIE color coordinate), except for the concurrent change in the emission intensities. The emission is very similar to that of the Ir(ppy)$_3$ (514 nm) [1], indicating that the trifluoromethyl group cannot affect the emission color greatly. The PL quantum yield of Ir(tfmppy)$_3$ in CH_2Cl_2 is 4.59% by reference to an aerated aqueous solution of [Ru(bpy)$_3$]Cl$_2$ (Φ=2.8%) as the standard solution. The Ir(tfmppy)$_3$ shows slightly red-shifted peak in the solid state under the UV light with emission maxima at 545 nm (green color, x=0.39, y=0.56) due to the rigidochromic effect.

2.3　Electrochemical property

To calculate the highest occupied molecular orbital (HOMO) and the lowest unoccupied molecular orbital (LUMO) levels of the Ir(tfmppy)$_3$ complex, the cyclic voltammogram was conducted using Ag/AgCl as the internal standard to investigate its electrochemical properties (Fig.3). Both quasi-reversible oxidation and reversible reduction process were observed in CH_2Cl_2 solution with 0.1 mol·L^{-1} n-Bu$_4$NClO$_4$ as supporting electrolyte. The HOMO energy level of Ir(tfmppy)$_3$

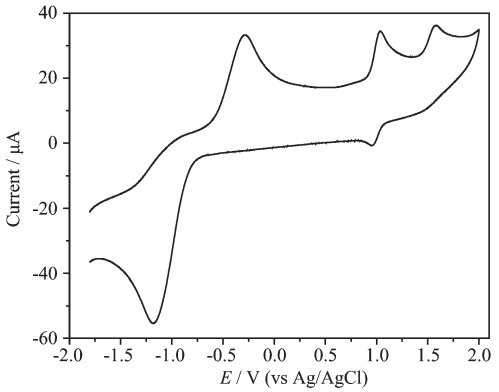

Fig.3 Cyclic voltammogram of $Ir(tfmppy)_3$ complex in CH_2Cl_2 solutions (1×10^{-3} mol·L^{-1})

relative to the vacuum level was calculated by using the oxidation potential and the Ag/AgCl energy level of −4.44 eV[29]. The band gap was obtained from the UV-Vis absorption spectra of $Ir(tfmppy)_3$. The LUMO energy level was calculated from the values of band gap and HOMO energy. On the basis of the potentials of the oxidation/reduction couples and the band gap, the HOMO/LUMO energy levels of $Ir(tfmppy)_3$ were estimated as −5.40/−2.80 eV.

2.4 Electroluminescence property

Energy level diagram of HOMO and LUMO levels (relative to vacuum level) for materials investigated in this work and their molecular structures are shown in Scheme 2. It is obvious that the HOMO and LUMO levels of $Ir(tfmppy)_3$ are within

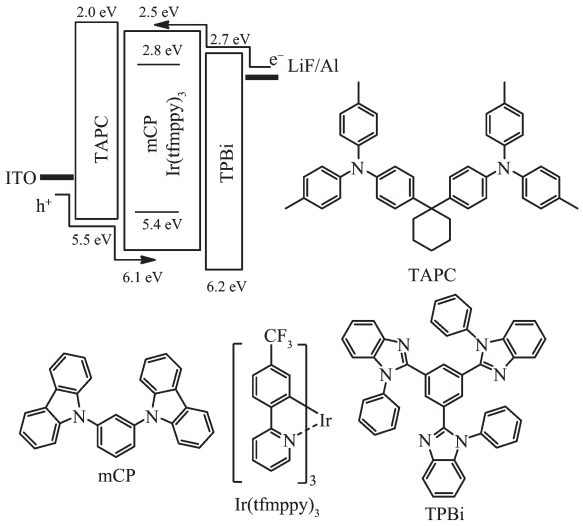

Scheme 2 Energy level diagram of HOMO and LUMO levels (relative to vacuum level) for materials investigated in this work

the HOMO and LUMO levels of mCP. Therefore, it is a good carrier trapping in these devices as expected and the carrier trapping may be the dominated EL mechanism. By adjusting the doping concentration of $Ir(tfmppy)_3$, two devices named as A (x=4%) and B (6%), respectively, were fabricated and investigated.

The EL spectra, voltage-luminance (V-L) characteristics, η_c and η_p versus J curves of the three devices are shown in Fig.4. All the devices have low turn-on voltage from 2.9 to 3.2 V with typical emission of $Ir(tfmppy)_3$ maxima at 515 nm, and a tiny residual emission from the host mCP at 381 nm[30] can be ignored. The CIE color coordinates are x=0.31, y=0.61, corresponding to the green region. The maximum luminance of device A based on 4% $Ir(tfmppy)_3$ reaches 43 612 cd·m^{-2} at 12.7 V with maximum η_c and η_p of 33.95 cd·A^{-1} (8.3 V) and 13.88 lm·W^{-1} (7.6 V), respectively. The driving voltages to reach the practical brightness of 100 and 1 000 cd·m^{-2} are 5.0 and 6.8 V, respectively. The device B with 6% $Ir(tfmppy)_3$ has a maximum luminance of 33 071 cd·m^{-2} at 9.6 V with a maximum η_c of 27.29 cd·A^{-1} (5.1 V) and a maximum η_p of 17.6 lm·W^{-1} (4.8 V), respectively. The EL performance of $Ir(tfmppy)_3$ complex are lower than those of $Ir(tfmppy)_2tpip$ previously reported by us[14]. For example, the device with 6% $Ir(tfmppy)_2tpip$ has a maximum luminance of 64 351 cd·m^{-2} at 11.8 V with a maximum η_c of 67.95 cd·A^{-1} and a maximum η_p of 69.90 lm·W^{-1}, respectively.

The EL efficiency increases with the increasing of current density until it reaches the maximum at 12.36 mA·cm^{-2} and 5.22 mA·cm^{-2} for device A and B, respectively. Afterwards, the EL efficiency decreases gradually with a further increase of current density. This phenomenon is called EL efficiency roll-off effect attributed to the triplet-triplet annihilation of the phosphor-bound excitons increasing[31] and field-induced quenching effects[17,30,32-33]. For device A, the η_c at the practical luminance of 100 cd·m^{-2} and 1 000 cd·m^{-2} is 9.82 and 27.70 cd·A^{-1}, respectively, and reaches the maximum current efficiency (33.95 cd·A^{-1}) at 4 197 cd·m^{-2}. For device B, the η_c at the practical luminance of 100 cd·m^{-2} and 1 000 cd·m^{-2} is 12.83

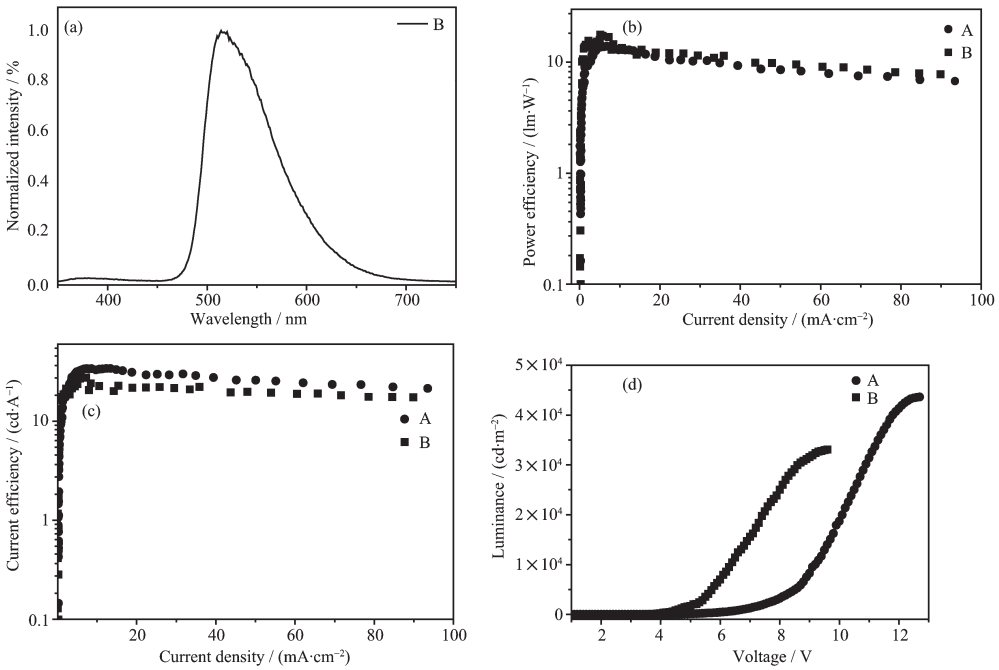

Fig.4　Characteristics of devices A and B: (a) EL spectra for device B, and (b) power efficiency as a function of current density, (c) current efficiency as a function of current density, and (d) V-L, current density and brightness versus voltage curves

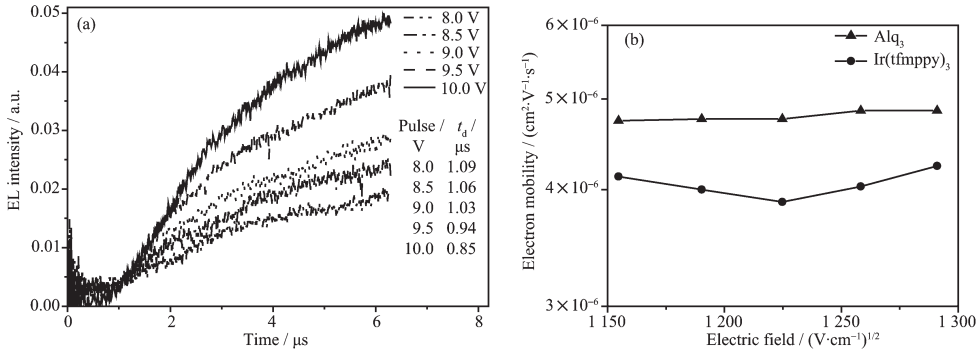

Fig.5　(a) Transient EL signals for the device structure of ITO/TAPC (50 nm)/Ir(tfmppy)$_3$ (60 nm) under different applied fields, and (b) Electric field dependence of charge electron mobility in the thin films of Alq_3 and Ir(tfmppy)$_3$

and 22.35 cd·A^{-1}, respectively, and reaches the maximum current efficiency (27.29 cd·A^{-1}) at 1 981 cd·m^{-2}.

The high efficiency of devices based on Ir(tfmppy)$_3$ can be interpreted by its better electron transport ability and shorter excite state lifetimes attributed to the more balanced injection and transport of carriers in (to) the emitting layer. To measure the electron mobility of Ir(tfmppy)$_3$, we conducted the transient EL measurement based on the device structure of ITO/TAPC (50 nm)/Ir(tfmppy)$_3$ (60 nm)[34]. The TAPC is the hole-transport layer while the Ir(tfmppy)$_3$ performs as both emissive and electron-transport layer. We select Alq_3 as a comparing material because it is the typically well-known electron transport material whose electron mobility has been reported in many references[34-36]. By comparing the Alq_3 electron mobility measured by us with the reported one, we can check the accuracy of our measurements. The experimental result shows that the electron mobilities in 60 nm Ir(tfmppy)$_3$ layer are between 3.88×10^{-6}~4.24×10^{-6} cm^2·V^{-1}·s^{-1} under electric field from 1 150 (V·cm^{-1})$^{1/2}$ to 1 300 (V·cm^{-1})$^{1/2}$. The result suggests that complex Ir(tfmppy)$_3$ has a comparable mobility to that of Alq_3 (4.74×10^{-6}~4.86×10^{-6} cm^2·V^{-1}·s^{-1}) as shown in Fig.5. The good electron transport ability

of $Ir(tfmppy)_3$ could balance the distribution of holes and electrons. The balanced hole and electron transporting ability will strengthen the recombination probability of electrons and holes, broaden the recombination zone, and reduce leakage current in the devices, which makes the devices exhibit relatively high efficiency and brightness at high current density.

3 Conclusions

In conclusion, $Ir(tfmppy)_3$ has been prepared and applied in the OLEDs of ITO/TAPC (60 nm)/$Ir(tfmppy)_3$:mCP (x%, 30 nm)/TPBi (60 nm)/LiF (1 nm)/Al (100 nm). For the device with x=4%, the device attains a maximum luminance 43 616 $cd \cdot m^{-2}$, a maximum η_c and η_p of 33.95 $cd \cdot A^{-1}$ and 13.88 $lm \cdot W^{-1}$, respectively. The electron mobility in $Ir(tfmppy)_3$ film reaches as high as that in Alq_3. We believe that the good electron mobility of the phosphorescent emitter results in the high devices efficiency at high brightness.

References:

[1] Tsuboyama A, Iwawaki H, Furugori M, et al. *J. Am Chem. Soc.*, **2003**,**125**:12971-12979

[2] Okada S, Okinaka K, Iwawaki H, et al. *Dalton Trans.*, **2005**, **9**:1583-1590

[3] Baldo M A, Lamansky S, Burrows P E, et al. *Appl. Phys. Lett.*, **1999**,**75**:4-5

[4] Holmes R J, Forrest S R, Tung Y J, et al. *Appl. Phys. Lett.*, **2003**,**82**:2422-2423

[5] Tokito S, Iijima T, Suzuri Y, et al. *Appl. Phys. Lett.*, **2003**, **83**:569-570

[6] Adachi C, Baldo M, Thompson M E, et al. *J. Appl. Phys.*, **2001**,**90**:5048-5051

[7] Kawamura Y, Goushi K, Brooks J, et al. *Appl. Phys. Lett.*, **2005**,**86**:071104-071105

[8] Li J, Djurovich P I, Alleyne B D, et al. *Inorg. Chem.*, **2005**, **44**:1713-1727

[9] Zhou G J, Wong W Y, Yao B, et al. *Angew. Chem. Int. Ed.*, **2007**,**46**:1149-1151

[10]Lyu Y Y, Byun Y, Kwon O, et al. *J. Phys. Chem. B*, **2006**, **110**:10303-10314

[11]Chang C F, Cheng Y M, Chi Y, et al. *Angew. Chem. Int. Ed.*, **2008**,**47**:4542-4545

[12]Ho C L, Wong W Y, Wang Q, et al. *Adv. Funct. Mater.*, **2008**,**18**:928-937

[13]Sasabe H, Takamatsu J, Motoyama T, et al. *Adv. Mater.*, **2010**,**22**:5003-5007

[14]King K A, Spellane P J, Watts R J, *J. Am. Chem. Soc.*, **1985**,**107**:1431-1432

[15]Lamansky S, Djurovich P, Murphy D, et al. *J. Am. Chem. Soc.*, **2001**,**123**:4304-4312

[16]King K A, Spellane P J, Watts R J, *J. Am. Chem. Soc.*, **1985**,**107**:1431-1432

[17]Adachi C, Baldo M A, Forest S R, et al. *Appl. Phys. Lett.*, **2000**,**78**:170-171

[18]Tanaka D, Sasabe H, Li Y J, et al. *Jpn. J. Appl. Phys.*, **2007**,**46**:L10-L12

[19]Zhu M R, Ye T L, He X, et al. *J. Mater. Chem.*, **2011**,**21**: 9326-9329

[20]Chou H H, Cheng C H, *Adv. Mater.*, **2010**,**22**:2468-2471

[21]Dedeian K, Djurovich P I, Garces F O, et al. *Inorg. Chem.*, **1991**,**30**:1865-1867

[22]Sykes D, Tidmarsh I S, Barbieri A, et al. *Inorg. Chem.*, **2011**,**50**:11323-11339

[23]Yu Z T, Yuan Y J, Cai J G, et al. *Chem. Eur. J.*, **2013**,**19**: 1303-1310

[24]Zhu Y C, Zhou L, Li H Y, et al. *Adv. Mater.*, **2011**,**23**:4041 -4046

[25]Li H Y, Zhou L, Teng M Y, et al. *J. Mater. Chem. C*, **2013**, **1**:560-565

[26]Wang Y, Herron N, Grushin V V, et al. *Appl. Phys. Lett.*, **2001**,**79**:449-450

[27]Hung L S, Chen C H. *Mater. Sci. Eng. R.*, **2002**,**39**:143-222

[28]Chan I M, Cheng W C, Hong F C. *Appl. Phys. Lett.*, **2002**, **80**:13-14

[29]Wu M F, Yeh S J, Chen C T, et al. *Adv. Funct. Mater.*, **2007**,**17**:1887-1895

[30]Baldo M A, O′Brien D F, You Y, et al. *Nature*, **1998**,**395**: 151-154

[31]Baldo M A, Adachi C, Forrest S R. *Phys. Rev. B*, **2000**,**62**: 10967-10977

[32]Baldo M A, O′Brien D F, Thompson M E, et al. *Phys. Rev. B*, **1999**,**60**:14422-14428

[33]Kalinowski J, Stampor W, Me-zyk J, et al. *Phys. Rev. B*, **2002**,**66**:235321-235335

[34]Teng M Y, Zhang S, Jiang S W, et al. *Appl. Phys. Lett.*, **2012**,**100**:073303-073305

[35]Scher H, Montroll E W. *Phys. Rev. B*, **1975**,**12**:2455-2477

[36]Lee J, Chopra N, Eom S H, et al. *Appl. Phys. Lett.*, **2008**, **93**:123306-123308